

# LIGHTEST MSSM HIGGS BOSON PRODUCTION AND ITS TWO-PHOTON DECAY AT THE LHC\*

B. KILENG

*NORDITA, Blegdamsvej 17, DK-2100 Copenhagen Ø, Denmark*

P. OSLAND

*University of Bergen, Allégt. 55, N-5007 Bergen, Norway*

and

P.N. PANDITA

*North Eastern Hill University, Permanent Campus, Shillong 793022, India*

## ABSTRACT

We present an analysis of the production and two-photon decay of the lightest CP-even Higgs boson of the Minimal Supersymmetric Standard Model (MSSM) at the Large Hadron Collider (LHC). A rather general model is considered, without supergravity constraints. All parameters of the model are taken into account, we especially study the dependence of the cross section on the squark masses, on the bilinear parameter  $\mu$  and the trilinear supersymmetry breaking parameter  $A$ . Non-zero values of these parameters lead to significant mixing in the squark sector, and, thus, affect the masses of Higgs bosons through radiative corrections, as well as their couplings to squarks. The cross section times the two-photon branching ratio of  $h^0$  is of the order of 15–25 fb in much of the parameter space that remains after imposing the present experimental constraints on the parameters.

## 1. Introduction

The most important production mechanism for the neutral SUSY Higgs bosons<sup>1</sup> at the Large Hadron Collider (LHC) is the gluon fusion mechanism,  $pp \rightarrow gg \rightarrow h^0, H^0, A^0$ ,<sup>2</sup> and the Higgs radiation off top and bottom quarks.<sup>3</sup> Except for the small range in the parameter space where the heavy neutral Higgs  $H^0$  decays into a pair of  $Z$  bosons, the rare  $\gamma\gamma$  decay mode, apart from  $\tau\tau$  decays, is a promising mode to detect the neutral Higgs particles, since  $b$  quarks are hard to separate from the QCD background. It has been pointed out that the lightest Higgs could be detected in this mode for sufficiently large values of the mass of the pseudoscalar Higgs boson  $m_A \gg m_Z$ .<sup>4, 5</sup>

---

\*To appear in: *Proceedings of the Workshop: Quantum Systems: New Trends and Methods*, Minsk, Belarus, June 3–7, 1996; hep-ph/9608315

Here we present results of a recent study<sup>6</sup> of the hadronic production and subsequent two-photon decay of the lightest  $CP$ -even Higgs boson ( $h^0$ ) of the MSSM, which is valid for the LHC energy of  $\sqrt{s} = 14$  TeV, focussing on the case of intermediate-mass squarks. The case of heavier squarks has been discussed elsewhere.<sup>6, 7</sup> A related study has been presented by Kane et al.<sup>8</sup> They consider a model where parameters are related by supergravity, but otherwise chosen randomly within their allowed ranges. As mentioned, the gluon fusion mechanism is the dominant production mechanism of SUSY Higgs bosons in high-energy  $pp$  collisions throughout the entire Higgs mass range. We study the cross section for the production of the  $h^0$  and its decay, taking into account all the parameters of the Supersymmetric Standard Model. In particular, we discuss the dependence on the squark masses, and take into account the mixing in the squark sector, the chiral mixing. This also affects the Higgs boson masses through appreciable radiative corrections, and was previously shown to lead to large corrections to the rates.<sup>9</sup>

In the calculation of the production of the Higgs through gluon-gluon fusion, we include in the triangle graph all the squarks, as well as  $b$  and  $t$  quarks, the lightest quarks having a negligible coupling to the  $h^0$ . On the other hand, in the calculation of decay of the Higgs to two photons, we include in addition to the above, all the sleptons,  $W^\pm$ , charginos and the charged Higgs boson.

An important role is played in our analysis by the bilinear Higgs coupling  $\mu$ , which occurs in the Lagrangian through the term

$$\mathcal{L} = \left[ -\mu \hat{H}_1^T \epsilon \hat{H}_2 \right]_{\theta\theta} + \text{h.c.}, \quad (1)$$

where  $\hat{H}_1$  and  $\hat{H}_2$  are the Higgs superfields with hypercharge  $-1$  and  $+1$ , respectively. Furthermore, the Minimal Supersymmetric Model contains several soft supersymmetry-breaking terms. We write the relevant soft terms in the Lagrangian as follows<sup>10</sup>

$$\begin{aligned} \mathcal{L}_{\text{Soft}} = & \left\{ \frac{gm_d A_d}{\sqrt{2} m_W \cos \beta} Q^T \epsilon H_1 \tilde{d}^R - \frac{gm_u A_u}{\sqrt{2} m_W \sin \beta} Q^T \epsilon H_2 \tilde{u}^R + \text{h.c.} \right\} \\ & - \tilde{M}_U^2 Q^\dagger Q - \tilde{m}_U^2 \tilde{u}^{R\dagger} \tilde{u}^R - \tilde{m}_D^2 \tilde{d}^{R\dagger} \tilde{d}^R - M_{H_1}^2 H_1^\dagger H_1 - M_{H_2}^2 H_2^\dagger H_2 \\ & + \frac{M_1}{2} \{ \lambda \lambda + \bar{\lambda} \bar{\lambda} \} + \frac{M_2}{2} \sum_{k=1}^3 \{ \Lambda^k \Lambda^k + \bar{\Lambda}^k \bar{\Lambda}^k \}, \end{aligned} \quad (2)$$

(see also ref. [9]) with subscripts  $u$  (or  $U$ ) and  $d$  (or  $D$ ) referring to up and down-type quarks. The Higgs production cross section and the two-photon decay rate depend significantly on several of these parameters.

The Higgs production cross section and the two-photon decay rate depend on the gaugino and squark masses, the latter being determined by, apart from the soft-supersymmetry breaking trilinear coefficients ( $A_u$ ,  $A_d$ ) and the Higgsino mixing parameter  $\mu$ , the soft supersymmetry-breaking masses, denoted in eq. (2) by  $\tilde{M}_U$ ,  $\tilde{m}_U$  and  $\tilde{m}_D$ , respectively. For simplicity, we shall consider the situation where  $\tilde{M}_U =$

$\tilde{m}_U = \tilde{m}_D \equiv \tilde{m}$ , with  $\tilde{m}$  chosen to be 150 GeV for the first two generations,<sup>\*)</sup> and varied over the values 150, 250, 500 and 1000 GeV for the third generation. As discussed in ref. [6], it suffices to consider  $A$  positive and vary the sign of  $\mu$ .

In Sec. 2, we discuss the implications of the nonzero values of  $A$  and  $\mu$  on the Higgs masses, together with the constraints related to the other relevant masses. We then go on to study the cross sections and decay rates for the lighter CP-even Higgs boson in Sec. 3.

## 2. Constraints on the Parameter Space

In this section we describe in detail the parameter space relevant for the production and decay of the lightest Higgs boson at LHC, and the theoretical and experimental constraints on it before presenting cross sections and decay rates.

At the tree level, the masses of the CP-even neutral Higgs bosons are given by  $(m_{h^0} \leq m_{H^0})$ <sup>11</sup>

$$m_{H^0, h^0}^2 = \frac{1}{2} \left[ m_A^2 + m_Z^2 \pm \sqrt{(m_A^2 + m_Z^2)^2 - 4m_Z^2 m_A^2 \cos^2 2\beta} \right], \quad (3)$$

which are controlled by two parameters,  $m_A$  (the mass of the CP-odd Higgs boson) and  $\tan \beta$  ( $= v_2/v_1$ , where  $v_2$  and  $v_1$  are the vacuum expectation values of the two Higgs doublets). Indeed, the entire Higgs sector at the tree level can be described in terms of these two parameters alone. At the tree level, the mass of the lightest Higgs boson ( $m_{h^0}$ ) is bounded by  $m_Z$ . There are, however, substantial radiative corrections<sup>12</sup> to the CP-even neutral Higgs masses. The radiative corrections are, in general, positive, and they shift the mass of the lightest neutral Higgs boson upwards.<sup>12</sup> More recent radiative corrections to the Higgs sector<sup>13</sup> which are valid when the squark masses are of the same order of magnitude, have not been taken into account in our study.<sup>6</sup> As long as the “loop particles” are far from threshold for real production, the cross section does not depend very strongly on the exact value of the Higgs mass.

In order to simplify the calculations, we shall assume that all the trilinear couplings are equal,

$$A_u = A_d \equiv A. \quad (4)$$

Furthermore, we shall take the top-quark mass to be 175 GeV<sup>14</sup> in our numerical calculations. The parameters that enter the neutral CP-even Higgs mass matrix are varied in the following ranges:

$$\begin{aligned} 50 \text{ GeV} &\leq m_A \leq 1000 \text{ GeV}, & 1.1 \leq \tan \beta \leq 50.0, \\ 50 \text{ GeV} &\leq |\mu| \leq 1000 \text{ GeV}, & 0 \leq A \leq 1000 \text{ GeV}. \end{aligned} \quad (5)$$

---

<sup>\*)</sup>Increasing  $\tilde{m}$  to 500 GeV for the first two generations leads to an increase in the cross section times the two-photon decay rate of about 5%.

These values cover essentially the entire physically interesting range of parameters in the MSSM. However, not all of the above parameter values are allowed because of the experimental constraints on the squark, chargino and  $h^0$  masses. For low values of  $\tilde{m}$ , the lightest squark tends to be too light (below the most rigorous experimental bound of  $\sim 45\text{--}48\text{ GeV}^{15}$ ), or even unphysical (mass squared negative). The excluded

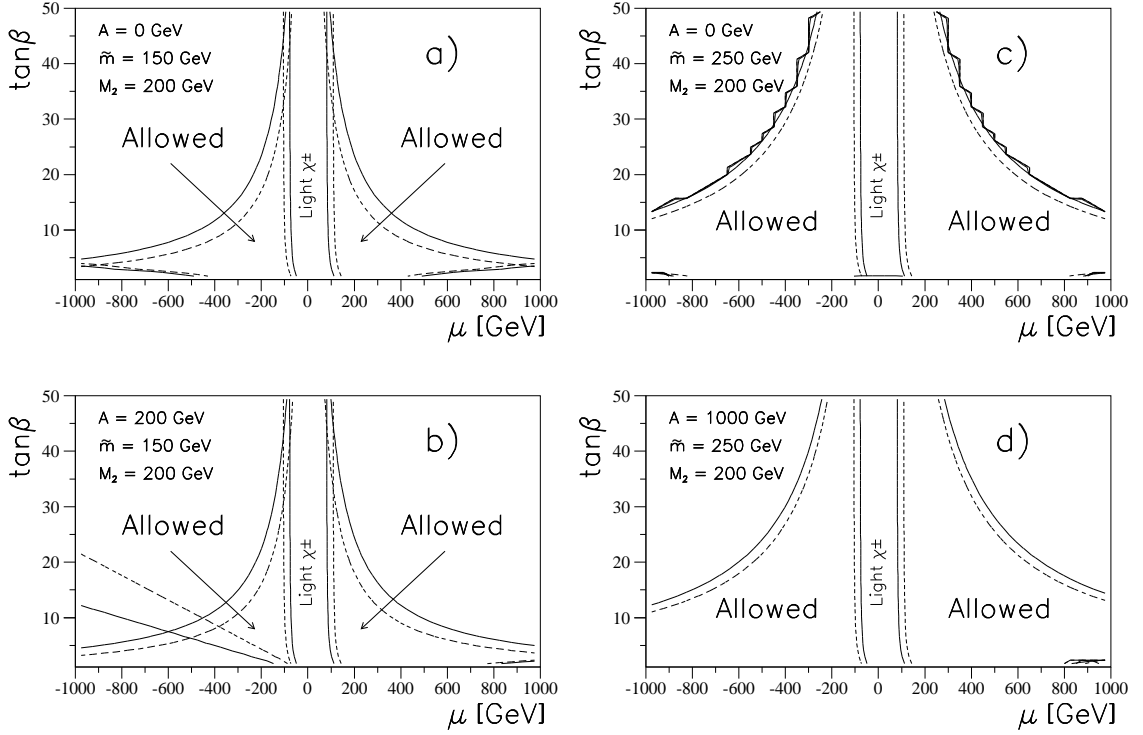


Figure 1. Regions in the  $\mu$ - $\tan\beta$  plane which are ruled out by too light chargino ( $\chi^\pm$ ) and squark masses. The gaugino mass scale is  $M_2 = 200\text{ GeV}$  and  $m_A = 200\text{ GeV}$ . The solid (dashed) contours for small  $|\mu|$  refer to the chargino mass  $m_{\chi^\pm} = 68$  (90) GeV. Two values of  $\tilde{m}$  are considered, left:  $\tilde{m} = 150\text{ GeV}$ , right:  $\tilde{m} = 250\text{ GeV}$ . For each value of  $\tilde{m}$ , two values of the trilinear mixing parameter are considered. For  $\tilde{m} = 150\text{ GeV}$ , the squark masses are too light or unphysical in much of the  $\mu$ - $\tan\beta$  plane. The hyperbola-like contours give regions that are excluded by the lightest  $b$  squark being below 45 GeV (solid) or 90 GeV (dashed). The more straight contours at large  $\mu$  and small  $\tan\beta$  similarly indicate regions that are excluded by the lightest  $t$  squark.

region of the parameter space is shown in the left part of fig. 1 for  $\tilde{m} = 150\text{ GeV}$ ,  $M_2 = 200\text{ GeV}$ ,  $m_A = 200\text{ GeV}$  and for two values of the trilinear coupling  $A$ . The allowed region in the  $\mu$ - $\tan\beta$  plane decreases with increasing  $A$ , but the dependence on  $M_2$  and  $m_A$  in this region is rather weak. In order to have acceptable  $b$ -squark masses,  $\mu$  and  $\tan\beta$  must lie *inside* of the hyperbola-shaped curves. Similarly, in order to have acceptable  $t$ -squarks, the corners at large  $|\mu|$  and small  $\tan\beta$  must be excluded.

The chargino masses are, at the tree level, given by the expression

$$m_{\chi^\pm}^2 = \frac{1}{2}(M_2^2 + \mu^2) + m_W^2 \pm \left[ \frac{1}{4}(M_2^2 - \mu^2)^2 + m_W^4 \cos^2 2\beta + m_W^2(M_2^2 + \mu^2 + 2\mu M_2 \sin 2\beta) \right]^{1/2}. \quad (6)$$

When  $\mu = 0$ , we see that, for  $\tan \beta \gg 1$ , the lightest chargino becomes massless. Actually, small values of  $\mu$  are unacceptable for all values of  $\tan \beta$ . The lowest acceptable value for  $|\mu|$  will depend on  $\tan \beta$ , but that dependence is rather weak. The excluded region due to the chargino being too light, increases with decreasing values of  $M_2$ . We note that the radiative corrections to the chargino masses are small for most of the parameter space.<sup>16</sup> In fig. 1 we show the contours in the  $\mu$ - $\tan \beta$  plane outside of which the chargino has an acceptable mass ( $> 68$  GeV)<sup>17</sup>. By the time the LHC starts operating, one would have searched for charginos with masses up to 90 GeV at LEP2. Contours relevant for LEP2 are also shown.

For  $\tilde{m} = 250$  GeV (right part of fig. 1), the region excluded due to low or unphysical squark masses is much reduced, and at  $\tilde{m} = 500$  GeV it is practically absent.<sup>6</sup> However, for larger values of  $\tilde{m}$  the experimental constraints on the  $h^0$  mass<sup>18</sup> rule out some corners of the  $\mu - \tan \beta$  plane.<sup>6</sup> The extent of these forbidden regions in the parameter space grow rapidly as  $m_A$  decreases below  $\mathcal{O}(150$  GeV). They also increase with increasing values of  $A$ .

As discussed above, the mass of the lighter  $CP$ -even Higgs boson  $h^0$  will depend significantly on  $\mu$ ,  $\tan \beta$ ,  $A$  and  $\tilde{m}$ , through the radiative corrections. For  $\tilde{m} = 250$  GeV, and two values each of  $m_A$  (100 and 200 GeV) and  $A$  (0 and 1000 GeV), the dependence on  $\mu$  and  $\tan \beta$  is displayed in fig. 2. At large  $|\mu|$  and large  $\tan \beta$ , the radiative corrections are large and negative, driving the value of  $m_{h^0}$  well *below* the tree-level value. (Those regions practically coincide with those where the  $b$  squarks are very light or unphysical.)

The charged Higgs boson mass is given by

$$m_{H^\pm}^2 = m_W^2 + m_A^2 + \Delta, \quad (7)$$

where  $\Delta$  arises due to radiative corrections and is a complicated function of the parameters of the model.<sup>19</sup>

The radiative corrections to the charged Higgs mass are, in general, not as large as in the case of neutral Higgs bosons. In certain regions of parameter space the radiative corrections can, however, be large. This is the case when the trilinear mixing parameter  $A$  is large,  $m_A$  is small, and when furthermore  $\tan \beta$  is large. We shall include the effects of non-zero  $A$  and  $\mu$  in the calculation of the charged Higgs mass. The present experimental lower bound of 40–45 GeV<sup>20</sup> on the charged Higgs is not restrictive, but presumably by the time the LHC starts operating, one will have searched for charged Higgs bosons at LEP2 with mass up to around 90 GeV. Even this bound does not appreciably restrict the parameter space.

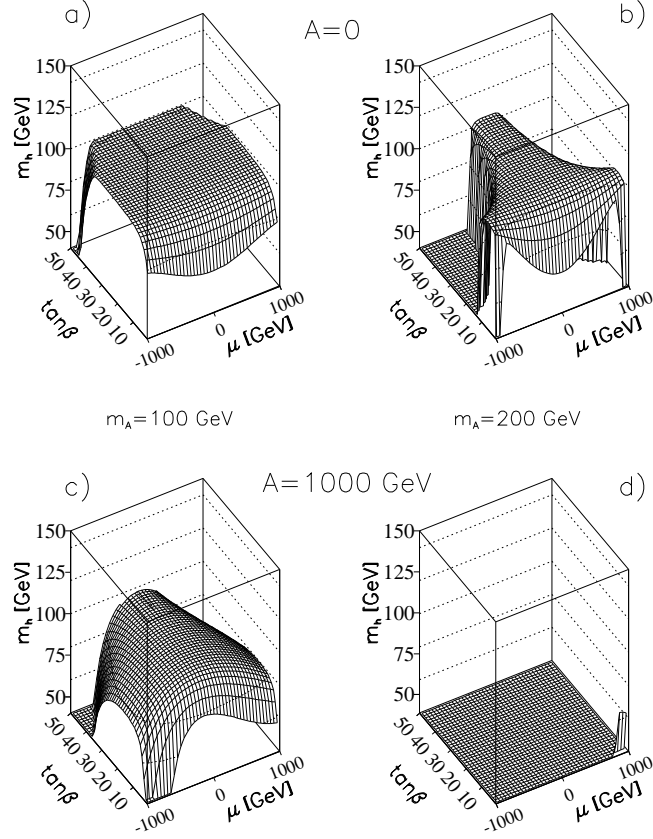


Figure 2. Mass of the lightest CP-even Higgs boson vs.  $\mu$  and  $\tan\beta$ , for  $M_2 = 200$  GeV and  $\tilde{m} = 250$  GeV. Two values of  $m_A$  and two values of  $A$  are considered: a)  $m_A = 100$  GeV,  $A = 0$ , b)  $m_A = 200$  GeV,  $A = 0$  GeV, c)  $m_A = 100$  GeV,  $A = 1000$  GeV, d)  $m_A = 200$  GeV,  $A = 1000$  GeV.

The neutralino mass matrix depends on the four parameters  $M_2$ ,  $M_1$ ,  $\mu$  and  $\tan\beta$ . However, one may reduce the number of parameters by assuming that the MSSM is embedded in a grand unified theory so that the SUSY-breaking gaugino masses are equal to a common mass at the grand unified scale. At the electroweak scale, we then have<sup>21</sup>  $M_1 = (5/3) \tan^2 \theta_W M_2$ . We shall assume this relation throughout in what follows. The neutralino masses enter the calculation through the total width of the Higgs boson. We here present numerical results for the gaugino mass parameter being  $M_2 = 200$  GeV. A wider range of values is considered in ref. [6]. The experimental constraints on the lightest neutralino mass rule out regions of the parameter space similar to those ruled out by the charginos.<sup>22</sup>

### 3. Cross Section and Two-Photon Decay

The cross section for  $pp \rightarrow h^0 X$ , is calculated from the triangle diagram convoluted with the gluon distribution functions,

$$\sigma = \sqrt{2} \pi G_F \left( \frac{\alpha_s}{8\pi} \right)^2 \frac{m_{h^0}^2}{s} \left| \sum_k I_k(\tau) \right|^2 \int_{-\log(\sqrt{s}/m_{h^0})}^{\log(\sqrt{s}/m_{h^0})} dy G\left(\frac{m_{h^0}}{\sqrt{s}} e^y\right) G\left(\frac{m_{h^0}}{\sqrt{s}} e^{-y}\right), \quad (8)$$

with contributions from various diagrams ( $k$ ). For the standard case of a top-quark loop,

$$I(\tau) = \frac{\tau}{2} \left\{ 1 - (\tau - 1) \left[ \arcsin\left(\frac{1}{\sqrt{\tau}}\right) \right]^2 \right\}, \quad (9)$$

and  $\tau = (2m_t/m_{h^0})^2 > 1$ .

For  $M_2 = 200$  GeV,  $\tilde{m} = 500$  GeV, and  $\mu = 500$  GeV, plots are given in refs. [6,7]. The following features are noteworthy:

- The cross section decreases appreciably for large values of  $A$ . This is mainly due to an increase in the  $h^0$  mass.
- The cross section increases sharply for small values of  $\tan \beta$ , and also at small  $m_A$ . The increase at small  $\tan \beta$  is caused by the  $h^0$  becoming light. At small values of  $m_A$  and large  $A$ , the couplings of  $h^0$  to  $b$  quarks and  $\tau$  leptons become large, making the cross section very large in this region.

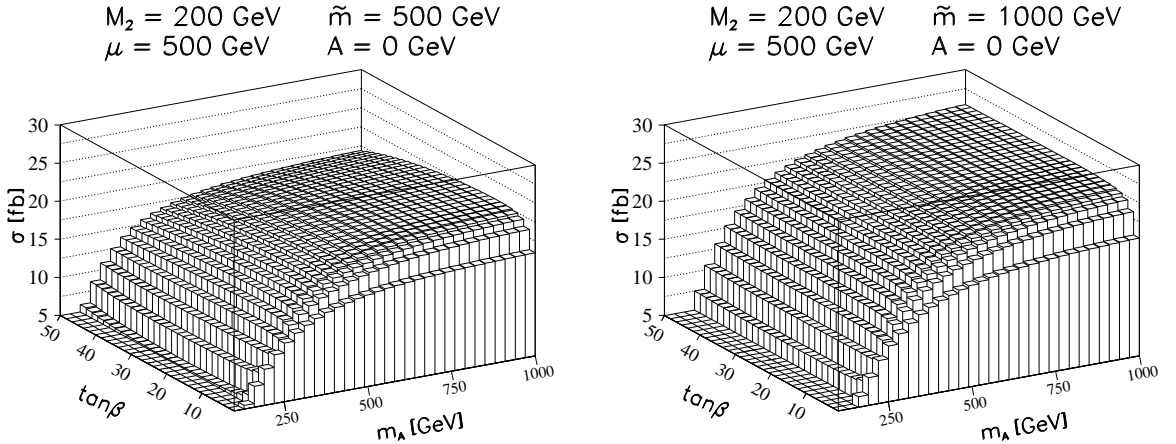


Figure 3. Cross section for  $pp \rightarrow h^0 X \rightarrow \gamma\gamma X$  as a function of  $m_A$  and  $\tan \beta$  for  $M_2 = 200$  GeV, two values of  $\tilde{m}$ : left:  $\tilde{m} = 500$  GeV, right:  $\tilde{m} = 1000$  GeV. For both cases,  $\mu = 500$  GeV, and  $A = 0$ .

The two-photon decay rate is found<sup>6, 7</sup> to increase sharply at large values of  $A$ , but this does not result in a correspondingly larger rate for the process

$$pp \rightarrow h^0 X \rightarrow \gamma\gamma X, \quad (10)$$

since the production cross section also decreases. In fig. 3 we show the cross section for the process (10) for the case of *heavy* squarks. A characteristic feature of the cross section is that it is small at moderate values of  $m_A$ , and then increases steadily with increasing  $m_A$ , reaching asymptotically a plateau. This behaviour is caused by the contribution of the  $W$  to the triangle graph for  $h^0 \rightarrow \gamma\gamma$ . The  $h^0 WW$  coupling is proportional to  $\sin(\beta - \alpha)$ , where

$$\cos^2(\beta - \alpha) = \frac{m_{h^0}^2(m_Z^2 - m_{h^0}^2)}{m_{A^0}^2(m_{H^0}^2 - m_{h^0}^2)}. \quad (11)$$

For large  $m_A$ , at fixed  $\beta$ , all Higgs masses, except  $m_{h^0}$ , become large, so that  $h^0$  decouples. For large  $m_A$ , we actually have  $\sin(\beta - \alpha) \rightarrow 1$ , which is why the cross section increases and reaches a plateau for large  $m_A$ .

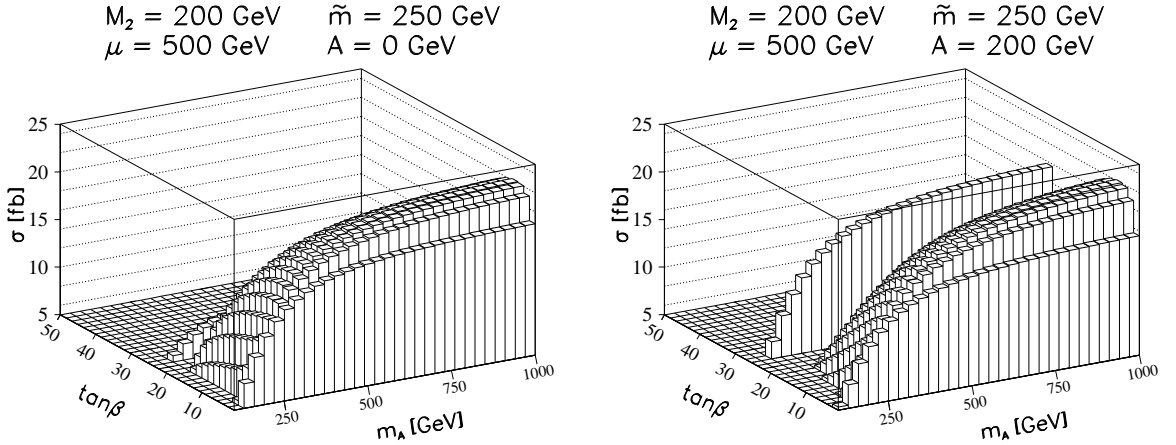


Figure 4. Cross section for  $pp \rightarrow h^0 X \rightarrow \gamma\gamma X$  as a function of  $m_A$  and  $\tan\beta$  for  $M_2 = 200$  GeV,  $\tilde{m} = 250$  GeV,  $\mu = 500$  GeV, and two values of  $A$ : left:  $A = 0$ , right:  $A = 200$  GeV.

The situation changes dramatically when we consider lighter squarks. In fig. 4 we show the corresponding cross section for the case of  $\tilde{m} = 250$  GeV. The main difference is that for large values of  $\tan\beta$  the product of the cross section and the two-photon decay rate practically vanishes. This is due to the fact that  $b$  squarks become light in this limit, the  $h^0$  can decay to  $b$  squarks, and the two-photon decay rate becomes too small.

For  $A = 200$  GeV, there is a band of larger values at  $\tan\beta \simeq 26$ . This region is rather “turbulent” (for these values of  $\tilde{m}$  and  $A$ ): As mentioned above, the two-photon decay rate vanishes due to decays to light  $b$  squarks, but at the same time the light Higgs tends to make the cross section big. The competition between these two effects is responsible for the turbulent behaviour seen here.



For some parameters, the latter effect may dominate, and we get spikes or bands in the product of the cross section and the two-photon decay rate. (Since a small Higgs mass is due to large radiative corrections—which are not accurately known—it is not clear how physical these bands or spikes are.)

The  $\mu$ -dependence of the cross section is for the case of  $M_2 = 200$  GeV and  $\tilde{m} = 500$  GeV discussed in refs. [6,7]. Here, for  $\tilde{m} = 250$  GeV, we show in fig. 5 the cross sections corresponding to those of fig. 4, but for  $\mu = -500$  GeV.

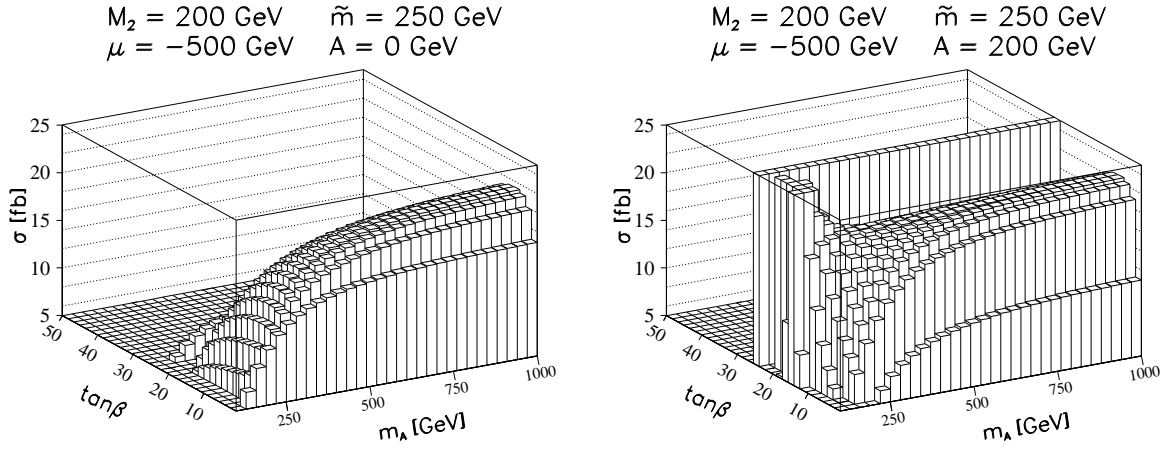


Figure 5. Cross section for  $pp \rightarrow h^0 X \rightarrow \gamma\gamma X$  as a function of  $m_A$  and  $\tan\beta$  for  $M_2 = 200$  GeV,  $\tilde{m} = 250$  GeV,  $\mu = -500$  GeV, and two values of  $A$ : left:  $A = 0$ , right:  $A = 200$  GeV.

#### 4. Summary and concluding remarks

We have discussed the cross section for the production of the lightest  $CP$ -even Higgs boson at the LHC, in conjunction with its decay to two photons. Where the parameters lead to a physically acceptable phenomenology, the cross section multiplied by the two-photon branching ratio for the lighter  $CP$ -even Higgs boson is of the order of 15–25 fb.

Similar results have been presented in ref. [8]. Within the context of a SUGRA GUT model, these authors consider basically a random sample of parameters compatible with experimental and theoretical constraints. The cross sections obtained in ref. [8] appear to be somewhat higher than those of ref. [6].

It should be noted that in regions where the Higgs cross section times the two-photon decay rate is small, typically the lightest  $b$  squark is light. Thus, as “compensation”, one should be able to observe  $b$  squarks.

The recent Fermilab data on large  $E_t$  inclusive jet cross sections<sup>23</sup> suggest that the gluon distribution functions are larger at high  $x$ .<sup>24</sup> We have checked whether these

distributions (specifically, CTEQ4HJ) lead to a higher rate for Higgs production. This turns out not to be the case. The enhancement of the gluon distribution function is in a range of  $x$  where its magnitude is simply too small, anyway.

These calculations do not take into account QCD corrections. Such corrections have been evaluated for the quark-loop contribution, and lead to enhancements of the cross section of about 50%.<sup>25</sup> For the squark loops QCD corrections have recently been studied using low-energy theorems.<sup>26</sup> It is concluded that the additional contributions lead to the same QCD corrections as for the top and bottom quark loops.

It is a pleasure to thank the Organizers of the Minsk Workshop, in particular Professor L. Tomil'chik, for creating a very stimulating and pleasant atmosphere during the meeting. This research has been supported by the Research Council of Norway. The work of PNP is supported by the Department of Science and Technology under project No. SP/S2/K-17/94.

## References

1. H.-P. Nilles, Phys. Rep. C110 (1984) 1;  
H. E. Haber and G. L. Kane, Phys. Rep. C117 (1985) 75;  
R. Barbieri, Riv. Nuovo Cimento 11 (1988) No. 4, p. 1;  
For a recent review, see, e.g., R. Arnowitt and P. Nath, Lecture at Swieca School, Campos do Jordao, Brazil, 1993; in *Sao Paulo 1993*, Proceedings, Particles and fields, 3-63; CTP-TAMU-93-052 and NUB-TH-3073-93, hep-ph/9309277.
2. H. M. Georgi, S. L. Glashow, M. E. Machacek, and D. V. Nanopoulos, Phys. Rev. Lett. 40 (1978) 692.
3. Z. Kunszt, Nucl. Phys. B247 (1984) 339;  
W. J. Marciano and F. E. Paige, Phys. Rev. Lett. 66 (1991) 2433;  
J. F. Gunion, Phys. Lett. B261 (1991) 510.
4. Z. Kunszt and F. Zwirner, Nucl. Phys. B385 (1992) 3.
5. H. Baer, M. Bisset, C. Kao and X. Tata, Phys. Rev. D46 (1992) 1067;  
V. Barger, M. S. Berger, A. L. Stange and R. J. N. Phillips, Phys. Rev. D45 (1992) 4128;  
J. F. Gunion and L. K. Orr, Phys. Rev. D46 (1992) 2052;  
V. Barger, Kingman Cheung, R. J. N. Phillips and A. L. Stange, Phys. Rev. D46 (1992) 4914.
6. B. Kileng, P. Osland and P. N. Pandita, Zeitschrift f. Physik C71 (1996) 87.
7. B. Kileng, P. Osland and P. N. Pandita, Invited paper, in *Xth International Workshop: High Energy Physics and Quantum Field Theory*, Proceedings of the conference, Zvenigorod, Russia, September 20–26, 1995, ed. B. Levtchenko, to appear; University of Bergen, Department of Physics Scientific/Technical Report No. 1996-01, ISSN 0803-2696, hep-ph/9601284.
8. G. L. Kane, G. D. Kribs, S. P. Martin, J. D. Wells, Phys. Rev. D53 (1996) 213.

9. B. Kileng, Zeitschrift f. Physik, C63 (1994) 87.
10. L. Girardello and M. T. Grisaru, Nucl. Phys. B194 (1982) 65.
11. J. F. Gunion, H. E. Haber, G. Kane and S. Dawson, *The Higgs Hunter's Guide*, Addison-Wesley, 1990.
12. Y. Okada, M. Yamaguchi, T. Yanagida, Prog. Theor. Phys. 85 (1991) 1; Phys. Lett. B262 (1991) 54;  
J. Ellis, G. Ridolfi and F. Zwirner, Phys. Lett. B257 (1991) 83; Phys. Lett. B262 (1991) 477;  
H. E. Haber and R. Hempfling, Phys. Rev. Lett. 66 (1991) 1815.
13. M. Carena, J. R. Espinosa, M. Quiros and C. E. M. Wagner, Phys. Lett. B355 (1995) 209.
14. CDF Collaboration, F. Abe, et al., Phys. Rev. Lett. 73 (1994) 225; *ibid.* 74 (1995) 2626; D0 Collaboration, S. Abachi, et al., Phys. Rev. Lett. 74 (1995) 2632.
15. DELPHI Collaboration, P. Abreu et al., Phys. Lett. B247 (1990) 148; OPAL Collaboration, R. Akers et al., Phys. Lett. B337 (1994) 207; ALEPH Collaboration, D. Buskulic, et al., Phys. Lett. B373 (1996) 246.
16. D. Pierce and A. Papadopoulos, Phys. Rev. D50 (1994) 565; Nucl. Phys. B430 (1994) 278;  
A.B. Lahanas, K. Tamvakis and N.D. Tracas, Phys. Lett. B324 (1994) 387.
17. ALEPH Collaboration, D. Decamp, et al., Phys. Lett. B236 (1990) 86; ALEPH Collaboration, D. Buskulic, et al., CERN PPE/96-086.
18. ALEPH Collaboration, D. Buskulic, et al., Phys. Lett. B313 (1993) 312; CERN PPE/96-079.
19. A. Brignole, J. Ellis, G. Ridolfi and F. Zwirner, Phys. Lett. B271 (1991) 123;  
A. Brignole, Phys. Lett. B277 (1992) 313;  
M. A. Diaz and H. E. Haber, Phys. Rev. D45 (1992) 4246.
20. ALEPH Collaboration, D. Buskulic, et al., Phys. Lett. B241 (1990) 623.
21. K. Inoue, A. Kakuto, H. Komatsu, S. Takeshita, Prog. Theor. Phys. 68(1982) 927, Erratum *ibid.* 70 (1983) 330; *ibid.* 71 (1984) 413.
22. R. Barbieri, G. Gamberini, G. F. Giudice and G. Ridolfi, Phys. Lett. 195B (1987) 500;  
J. Ellis, G. Ridolfi and F. Zwirner, Phys. Lett. 237B (1990) 423.
23. CDF Collaboration (F. Abe et al.), Phys. Rev. Lett. 77 (1996) 438.
24. H. L. Lai, et al., MSUHEP-60426 (Jun. 1996), hep-ph/9606399.
25. M. Spira, A. Djouadi, D. Graudenz and P. M. Zerwas, Nucl. Phys. B453 (1995) 17.
26. S. Dawson, A. Djouadi, M. Spira, Phys. Rev. Lett. 77 (1996) 16.
27. A. Djouadi, P. Janot, J. Kalinowski, P. M. Zerwas, Phys. Lett. B376 (1996) 220.